Effect of Cryogenic Temperature on the Fracture Toughness of Graphite/Epoxy Composites

S. G. Kalarikkal
Graduate Student

B. V. Sankar
Newton C. Ebaugh Professor
Fellow ASME
e-mail: sankar@ufl.edu

P. G. Ifju
Professor

Department of Mechanical and Aerospace Engineering,
University of Florida,
P.O. Box 116250,
Gainesville, FL 32611-6250

The research presented in this paper is an effort to better understand the interlaminar fracture behavior of graphite/epoxy composite laminates in cryogenic conditions. Double cantilever beam tests were performed on different types of specimens, at room and cryogenic temperatures, and the fracture toughness was calculated from their load-displacement diagram. Additionally, the fracture toughness of some plain-weave textile composite specimens and specimens treated with nanoparticles (38 nmAl_2O_3) *were also measured. It was observed that all specimens, with the exception of woven composites, showed deterioration in fracture toughness at the liquid nitrogen temperature. Nanoparticle treated specimens showed an improvement in fracture toughness, both at room and cryogenic temperatures compared to the control specimens. The woven composite specimens showed an increase in fracture toughness at cryogenic temperature. The results indicate that woven fiber composites may have potential in lightweight cryogenic storage systems.* [DOI: 10.1115/1.2172274]

Introduction

Fiber reinforced composites, due to their high stiffness to weight ratio and strength to weight ratio, are being considered for liquid hydrogen (LH_2) fuel tank structures in future space vehicles. Tests have shown that graphite/epoxy composites have a tendency to microcrack at very low temperatures. In the case of fuel tanks, these microcracks can act as passages for the cryogenic fuel to permeate, which could ultimately lead to the failure of the whole structure [1,2]. Hence, it is very important that we understand the fracture behavior of fiber composites at cryogenic temperatures before they are used in cryogenic storage systems.

Earlier researchers focused on the effect of higher temperatures on the fracture behavior of graphite/epoxy composites. Very little research has been done to determine the low temperature response of composites. The goal of this paper is to determine the effect of cryogenic temperature on the delamination resistance of graphite/epoxy composite laminates. Furthermore, techniques to improve the fracture toughness at cryogenic conditions are also explored. Linear elastic fracture mechanics (LEFM) has been successfully used to characterize the delamination resistance of fiber composite materials [3]. The double cantilever beam specimen (DCB) is simple to fabricate, and the test is quite repeatable and easy to perform. Hence we have chosen the DCB test to determine the fracture toughness at cryogenic temperature, and compare with results from room temperature tests.

Sankar and Sonik [4], and Sun and Zheng [5] analyzed the distribution of the strain energy release rate (G) at the crack fronts of DCB specimens using plate finite elements. They found a boundary layer phenomenon in the distribution of G at the crack front, which causes the strain energy release rate to vary along the straight crack front. They concluded that beam theory underestimated the strain energy release rate for a curved crack front, which is actually observed in the actual test specimens. They also found that for laminated composites containing angle plies the distribution of G is skewed and the skewness depends on the lay-up sequence.

The effect of stacking sequence on the strain energy release rate across the specimen width for DCB specimens was determined by Davidson et al. [6]. They investigated eight different stacking sequences, with cracks between 30 deg/30 deg and 30 deg/−30 deg interfaces. They found that all specimens exhibited an asymmetry in the distribution of the energy release rate about the center of the specimen's width. They concluded that the difference in G was more important than the small asymmetry.

Mode I interlaminar fracture of carbon/epoxy cross-ply composites was investigated by de Morais et al. [7] and de Morais [8]. They performed mode I DCB tests on carbon/epoxy $[0\text{ deg}/90\text{ deg}]_{12}$ specimens with the starter crack between the 0 deg and 90 deg midlayer. They observed that the crack propagated along the neighboring 0 deg/90 deg interface and within the 90 deg midlayer. They measured the interlaminar critical strain energy release rate using a corrected beam theory and found that the intralaminar fracture toughness (G_c) is significantly smaller than the interlaminar G_c. This would prevent pure interlaminar propagation in multidirectional specimens with high interlaminar fracture toughness. Using an interlaminar stress based criterion, de Morais [8] predicted that G_c of multidirectional specimens is typically 10–40% higher than G_c of unidirectional laminates.

Ashcroft et al. [9] conducted mode I constant displacement rate test on epoxy bonded carbon fiber reinforced plastic (CFRP) joints at −50°C, 22°C, and 90°C. They observed that the temperature influenced the mode of fracture which progresses from stable, brittle fracture at low temperature to slip-stick fracture at room temperature and finally to stable ductile fracture at elevated temperatures. They also observed an increase in strain energy release rate with temperature.

Shindo et al. [10] performed DCB tests on SL-E woven glass-epoxy laminates at room temperature, liquid nitrogen (LN_2) temperature, and liquid helium temperature to evaluate the effect of temperature on the interlaminar fracture toughness. They determined the Mode I critical strain energy release rate using the modified compliance calibration (MCC) method and area method. They observed that the specimens tested at room temperature were characterized by stable crack propagation while the specimens tested at LN_2 temperature and liquid helium temperature were characterized by load peaks at which unstable fracture occurred. They also found that the interlaminar fracture toughness increased between room temperature and LN_2 temperature, and a decrease in fracture toughness on further cooling to liquid helium temperature.

Contributed by the Materials Division of ASME for publication in the JOURNAL OF ENGINEERING MATERIALS AND TECHNOLOGY. Manuscript received January 20, 2005; final manuscript received October 25, 2005. Review conducted by Assimina Pelegri.

Table 1 Specimen designation and layup

Crack between	Specimen ID	Layup	Number of plies
0 deg plies	0D0	$[(0/90)_4/0/D]_s$	18
90 deg plies	90D90	$[(90/0)_4/90/D]_s$	18
0 deg and 90 deg plies	90D0	$[(0/90)_4/D/0(90/0)_4]$	17
Two 0 deg plies with 20% nanoparticle	0D0_N_20	$[(0/90)_4/0/D]_s$	18
Two 0 deg plies with 9% nanoparticle	0D0_N_9	$[(0/90)_4/0/D]_s$	18
Plain Woven composite	TEX		12

There are several different methods for increasing the delamination resistance of fiber reinforced composite laminates. Most of these methods employ the introduction of translaminar reinforcement in the composite by stitching [11] or by inserting pins called z pins [12,13]. The introduction of nanoparticles such as aluminum oxide or zinc oxide in the composite laminate is an emerging technique to improve the structural property of the laminates including the delamination resistance.

Wu et al. [14] investigated the mechanical, thermal, and morphological properties of glass fiber and carbon fiber reinforced polyamide-6 and polyamide-6/clay nanocomposites. They found that the effect of nanoscale clay on toughness was more significant than that of the fiber. Other researchers like Becker, Varley, and Simon [15] also experimented with the use of layered silicates to enhance the fracture toughness of high performance carbon epoxy composites. They found that the use of layered silicates increased the maximum load by about 25% along with a 50% increase in the critical strain energy release rate.

Timmerman et al. [16] modified the matrices of carbon fiber/epoxy composites with layered inorganic clays and traditional filler and determined the micro- and nano-scale response of the material to cryogenic cycling. They observed that the mechanical behavior was not significantly altered by the modification and that the incorporation of nanoclay reinforcement in proper concentrations resulted in laminates with microcrack densities lower than the unmodified material as a response to cryogenic cycling.

The objective of this paper is to determine the Mode I fracture behavior of graphite/epoxy composite laminates at cryogenic temperatures by using the DCB test. This paper also explores techniques to improve the fracture toughness of these composites by the use of nanoparticles and textile composites.

Experimental Procedure

Specimen Fabrication. ASTM-D 5528-94a test method [17] was followed to fabricate the test specimens. The unidirectional composite laminate specimens were fabricated from Toray Composites T800-3631 prepreg (material designation A50TF266 S6 Class E, Fiber designation T800HB-12K-40B, matrix 3631) while the textile laminate specimens were prepared using the SP Systems SE 84 prepreg. Each specimen was 178 mm (7 in.) in length; 25 mm (1 in.) in width, and approximately 3 mm (0.12 in.) in thickness [18]. Different sets of unidirectional laminate specimens were fabricated with the precrack between two 0 deg plies, two 90 deg plies, between a 0 deg ply and a 90 deg ply, and between two plain weave textile plies. Table 1 shows the specimen designation, layup and the number of plies in each specimen. The "D" in the layup signifies the position of pre-crack or delamination. In the rest of the paper "0D0" will be used to refer to the specimen with precrack between two 0 deg plies, "90D90" denotes the specimen with precrack between two 90 deg plies and so on. The precrack was created in the laminates by placing a Teflon™ film at one end of the panel between the designated plies. Details of specimen fabrication can be found in [18].

The interlaminar surfaces of some of the specimens were treated with nanoparticles (38 nmAl_2O_3) to study its effect on the fracture toughness. The nanoparticles were mixed with isopropyl alcohol and a thin layer of the solution was uniformly coated on the plies before laying them up. Two sets of specimens were prepared by this method by varying the mass of the nanoparticles coated between the plies. The mass of the nanoparticles coated was, respectively, 9% and 20% of the mass of a single ply of the composite. The 9% nanoparticle impregnated specimen will be represented by 0D0_N_9, and 0D0_N_20 will be used to refer to the 20% nanoparticle composite.

In addition to tape laminates some plain weave textile laminate specimens were also fabricated to determine the effect of cryogenic temperature on their fracture toughness. The textile composite laminates used 12 plies and their mass was approximately equal to that of unidirectional composite specimens. In the following the textile specimens will be denoted by "TEX."

Vacuum bagging method was used to cure the composite specimens in an autoclave. The unidirectional and textile composites were cured at 180°F (355°F) and 132°F (270°F), respectively. A vacuum of 30 Hg was applied during the cure cycle. The specimens were wet cut to dimension with a diamond saw after the

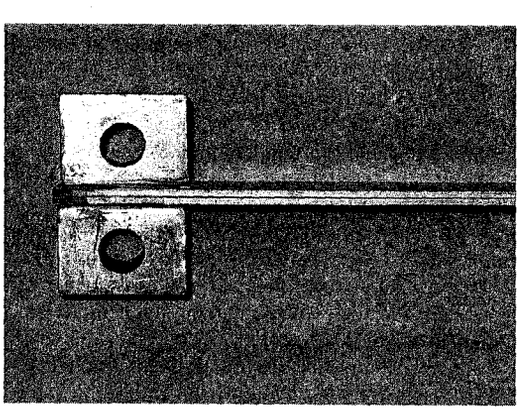

Fig. 1 DCB specimen with the loading blocks attached

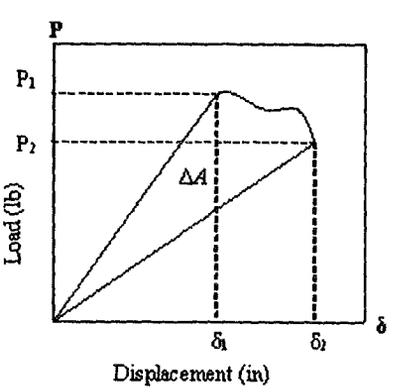

Fig. 2 DCB test load-displacement diagram

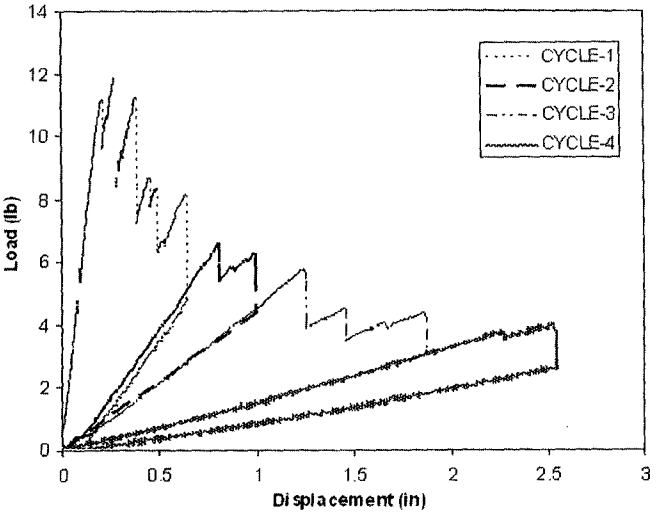

Fig. 3 Typical room temperature DCB test load-displacement diagram

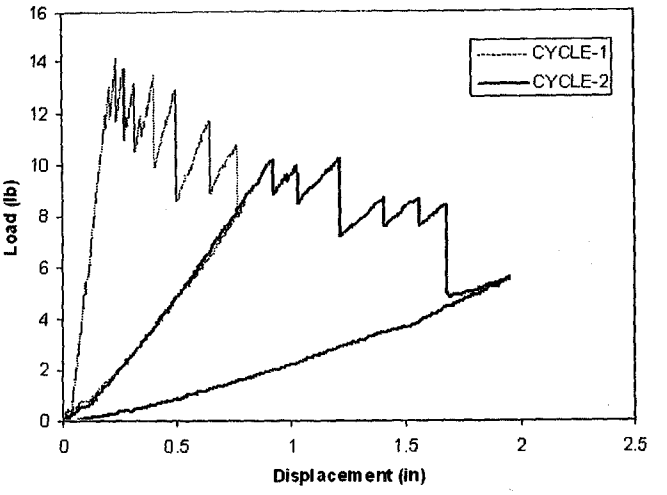

Fig. 4 Typical cryogenic temperature DCB test load-displacement diagram

curing process.

Two loading blocks were attached to the DCB specimens for applying the opening force. Figure 1 shows the DCB specimen with the loading blocks attached. The loading blocks were fabricated from a rectangular steel bar. The dimensions of the loading blocks were $28 \times 20 \times 15$ mm ($1.1 \times 0.8 \times 0.6$ in.). A 9.5 mm (3/8-in.) hole was drilled through the center of each loading block to allow the insertion of a loading pin. Epoxy 907 manufactured by the Miller-Stephenson chemical company was used as the adhesive to attach the loading blocks to the DCB specimens for the room temperature tests and PR-1665 cryogenic adhesive from PRC-DeSoto International was used for the cryogenic test.

Epoxy 907 is a two part adhesive. Equal parts by volume of part A and part B were mixed thoroughly for 3 min on a clean surface. A thin layer of the mixed adhesive was then applied evenly on the loading blocks. The loading blocks were then mounted on the composite specimen. Pressure was applied on the blocks to squeeze out excess adhesive to form a thin glue line. The excess adhesive was removed with a knife. Great care was taken while mounting the loading block to ensure symmetry of the specimen. The adhesive was allowed to cure for 24 h at 24°C.

PR-1665 is a high tear and tensile strength cryogenic potting and molding compound. It is supplied in a two-part kit, Part A and Part B. Part A was heated to 125°C with constant stirring and allowed to cure before using. Part B was also heated to 60°C with constant stirring and was cooled before mixing. 35:100 ratio parts by volume of Part A and Part B was mixed thoroughly using a mixing paddle. The mixed adhesive is then applied uniformly on the loading blocks, which were then mounted on the composite specimens. A small pressure was applied on the loading blocks to squeeze out the excess adhesive which were then removed with a knife. The adhesive was then cured for 24 h at 24°C and 40 h at 54°C.

Fracture Tests. The Mode I DCB test was used to determine the delamination resistance of the composite laminates. A displacement controlled DCB test gives rise to stable crack growth, which makes it ideal to measure the Mode I fracture toughness G_{Ic}. The critical strain energy release rate can be calculated from the load-displacement diagram (Fig. 2) of the DCB test. In this study the fracture toughness was calculated using the area method.

The fracture toughness is given by

$$G_c = \frac{\Delta A}{B\Delta a} \tag{1}$$

where ΔA is the area between the loading and unloading curves, Δa is the crack extension, and B is the width of the specimen.

Room Temperature Tests. The DCB tests were conducted in a 12,000 lb MTI universal testing machine with a 5000 lb interface load cell. The tests were performed at a crosshead displacement rate of 1 mm/min (0.04 in./min) to simulate a quasistatic condition. For the room temperature (24°C±2°C) tests, each specimen was cyclically loaded and unloaded four times. The crack was allowed to propagate approximately by 25 mm (1 in.) during each loading cycle and was then unloaded. Figure 3 shows a typical loading and unloading cycle. Once the crack propagates to a distance of about 25 mm, the crosshead was held at hold and the tip of the crack was marked with a sharp-tipped marker before unloading. This mark indicates the tip of the initial crack for the next

Table 2 Room temperature fracture toughness results

Specimen	No. of specimens tested	No. of loading-unloading cycle on each specimen	Fracture Toughness G_{Ic} N/m (lb/in.)	Coefficient of variation (%)	Percentage change with respect to 0D0 specimen (%)
0D0	2	4	225 (1.28)	7.20	-
90D90	2	4	395 (2.25)	8.63	75
90T0	2	4	177 (1.01)	10.34	-21
0D0_N_20	2	4	216 (1.23)	15.07	-4
0D0_N_9	2	4	443 (2.53)	9.50	97
TEX	2	4	422 (2.41)	10.02	88

loading cycle. The process was repeated during each loading cycle. The crack growth was monitored using a microscope.

Cryogenic Temperature Tests. A cryogenic chamber was designed and fabricated to perform the DCB test at cryogenic temperature. Liquid nitrogen (LN_2), which boils at 77 K at atmospheric pressure, was used as the cryogen. The cryogenic chamber consisted of two concentric steel drums of diameters 457 mm (18 in.) and 356 mm (14 in.) with an insulated annulus. Styrofoam sheets were used as the insulating material. The outer drum was also insulated to reduce the boil off of LN_2. The fixtures for the DCB test were fastened to a bottom shaft, which was screwed to the MTI machine. Although the steel chamber was leak proof, three polyethylene bags were used to cover the inside of the chamber as an additional safety measure.

The in situ DCB test was performed by keeping the DCB specimen fully immersed in the LN_2 bath throughout the loading-unloading cycle to ensure uniform temperature distribution in the specimen. LN_2 was supplied at a constant rate to compensate for the loss due to boiling. The specimens were kept immersed in the LN_2 bath for 30 min before starting each loading cycle.

The cryogenic tests were performed at the same loading (1 mm/min) as the room temperature tests. Since the DCB specimen is immersed in the LN_2 bath during testing, it was not possible to monitor the crack growth. Hence each specimen was removed from the LN_2 after each loading and unloading cycle. The distance through which the crack propagated was measured using the microscope and the crack tip was marked with a sharp tipped marker on both sides of the DCB specimen. The specimen was again mounted and the test was repeated. Each specimen underwent two loading-unloading cycles. Figure 4 shows a typical loading-unloading cycle at cryogenic temperature.

The fracture toughness (G_{Ic}) was calculated for each specimen at room and cryogenic temperature using the area method and the results were compared.

Results and Discussions

Room Temperature Tests. Table 2 shows the average G_{Ic} values of two specimens (eight cycles) at room temperature for each specimen type. The comparison of unidirectional laminated specimens, 0D0 and 90D90, shows that the fracture toughness of 90D90 specimens (395 N/m) is greater than that of 0D0 specimens (225 N/m). In a DCB test, the crack grows along the path of least resistance. In the case of the 0D0 specimens there exists a plane containing only resin, and the crack propagates along this plane. The fibers in the case of the 90D90 specimen act as barriers for the crack to propagate. In such a situation, the crack has to go around the fibers, creating a much larger surface area, and hence the higher fracture toughness. The crack propagation was observed to be both intralaminar and interlaminar in the 90D90 specimens. The crack followed a zigzag route, traveling from one 0/90 interface to the other 0/90 interface adjacent to the pre-crack. The 90D0 specimen, with the crack between a 90 deg ply and a 0 deg ply showed the least resistance (177 N/m) to crack propagation. It was observed that the crack stayed on the interface of the two plies and did not jump as in the case of the 90D90 specimen. The 9% nanoparticle treated specimen shows the highest delamination resistance (443 N/m) compared to all the other specimen types. The reason might be due to the fact that the nanoparticles act as a barrier for crack propagation, and hence the crack has to pass around the nanoparticles, thereby increasing the energy required for crack growth. The 20% nanotreated specimen showed poorer fracture toughness (216 N/m) compared to the non-nano 0D0 specimen. The reason for the poor performance of the 0D0_N_20 specimen might be due to the possible agglomeration of the nanoparticles, which might have hindered the adhesion of the plies during cure. Figure 5 shows the scanning electron microscope (SEM) image of the crack surface of the 20% nanotreated specimen. We can clearly see that the nanoparticles are not uniformly distributed on the surface and there are areas of high and low concentration of the nanoparticle.

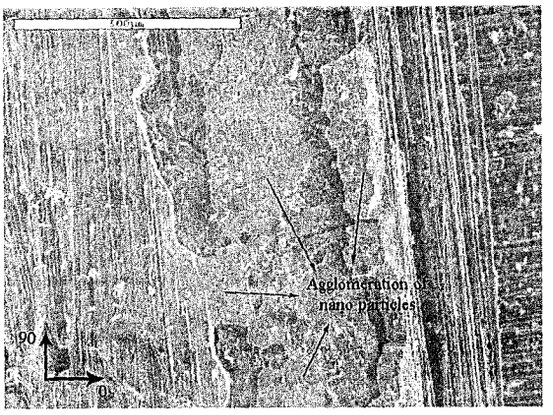

Fig. 5 SEM image of 20% nanotreated specimen crack surface

The textile specimens also showed higher fracture toughness (422 N/m) compared to 0D0 specimens. In fact, it shows the second highest fracture toughness next to the 0D0_N_9 specimen at room temperature. As in the case of 90D90 specimens the textile laminates do not have a plane containing only resin. The crack has to propagate around the fiber yarns creating a much larger fracture surface area.

Cryogenic Temperature Tests. Table 3 shows the average G_{Ic} values at cryogenic temperature for each specimen type. It is seen that the fracture toughness of the unidirectional composite specimens 0D0 and 90D90 deteriorate significantly at cryogenic temperature. The 0D0 specimen has a fracture toughness of 164 N/m at cryogenic temperature and that of 90D90 specimen is 236 N/m. The decrease in fracture toughness might be due to the development of thermal stresses in the laminate and formation of

Table 3 Cryogenic temperature fracture toughness results

Specimen	No. of specimens tested	No. of loading-unloading cycle on each specimen	Fracture toughness G_{Ic} in N/m (lb/in.)	Coefficient of variation (%)	Percentage change with respect to 0D0 specimen (%)
0D0	2	2	164 (0.94)	22.32	-
90D90	2	2	236 (1.34)	14.95	44
90T0	2	2	173 (0.99)	42.32	5
0D0 20% nano	2	2	189 (1.08)	11.92	16
0D0 9% nano	2	2	251 (1.43)	19.15	53
TEX	2	2	827 (4.72)	6.19	404

Table 4 Effect of cryogenic temperature on fracture toughness

Specimen	Fracture toughness G_{Ic} in N/m (lb/in.)		Change with respect to room temperature G_{Ic} (%)
	Room temperature	Cryo temperature	
0D0	225 (1.28)	164 (0.94)	−27
90D90	395 (2.25)	236 (1.34)	−40
90T0	177 (1.01)	174 (0.99)	−2
0D0 20% nano	216 (1.23)	189 (1.08)	−12
0D0 9% nano	443 (2.53)	251 (1.43)	−43
TEX	422 (2.41)	827 (4.72)	96

microcracks in the laminate at the low temperature, which leads to overall degradation of the material as well as embrittlement of the matrix.

The nanotreated specimens too showed a decrease in fracture toughness at the cryogenic temperature. Although the fracture toughness of 0D0_N_9 composite dropped at cryogenic temperature (from 443 N/m to 251 N/m), it is still higher than the room temperature G_{Ic} of 0D0 (251 N/m) and also higher than cryogenic temperature G_{Ic} of 90D90 composite (236 N/m).

The textile specimens showed the most interesting behavior at cryogenic temperature. From Table 3 we can see that the fracture toughness of the TEX specimen increased from 427 N/m at room temperature to (827 N/m) at cryogenic temperature. It was observed that the crack does not propagate in one plane but traverses through the different plies.

Comparison of Room and Cryogenic Test Results

Effect of Layup on G_{Ic}. Table 4 shows the comparison of the fracture toughness at room and cryogenic temperatures. Comparing the fracture toughness of the 0D0 and the 90D90 composites, it can be seen that the fracture toughness decreases by 27% and 40%, respectively, compared to the room temperature specimens. It is also observed that the fracture toughness of the 90D90 specimen at cryogenic temperature is higher than the fracture toughness of the 0D0 specimen at room temperature. Figure 6 shows the comparison of the fracture toughness of the two unidirectional specimens.

Figures 7 and 8 show the 0D0 and 90D90 crack surfaces. We can see that in the case of the 0D0 specimen the crack stays in its initial plane while the crack growth in 90D90 is not planar but it takes a tortuous path moving between adjacent plies. As mentioned earlier the increase in fracture energy in the case of 90D90 specimens might be due to this translaminar crack path.

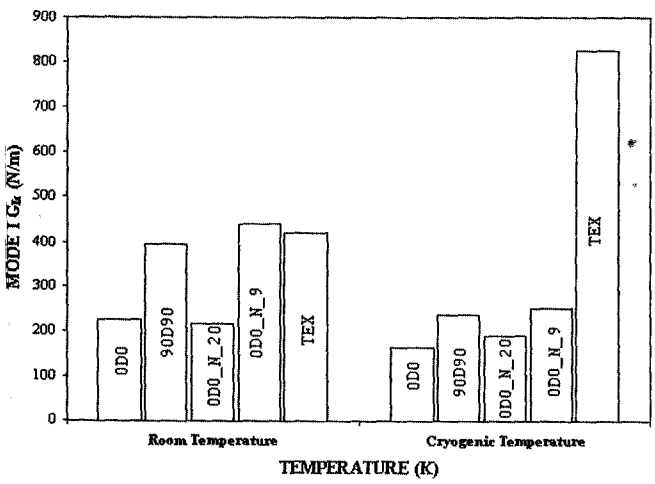

Fig. 6 Comparison of G_{Ic} for various laminates

Effect of Nanoparticles on G_{Ic}. It was observed that the fracture toughness of 9% nanoparticle treated composite was higher (443 N/m and 251 N/m) than the non-nano 0D0 specimens (225 N/m and 164 N/m) at both room and cryogenic temperatures. The nanoparticles probably act as an obstruction to the propagation of the crack. The impregnation of 9% nanoparticles increases the fracture toughness by nearly 97% at room temperature and by 53% at cryogenic temperature. Also, the fracture toughness of the 0D0_N_9 specimens at cryogenic temperature (251 N/m) is higher than the fracture toughness of the non-nano 0D0 specimen (225 N/m) at room temperature. From Fig. 6, it can be observed that the fracture toughness of the 0D0_N_9 specimen is very similar to the 90D90 specimens. Figure 9 shows the SEM photograph of the 0D0_N_9 specimen crack surface. At this magnification we cannot see much difference between the 0D0_N_9 specimen and the 0D0 specimen (Fig. 7) crack surface. A more magnified view of the crack surfaces is required to study

Fig. 7 SEM image showing 0D0 specimen crack surface

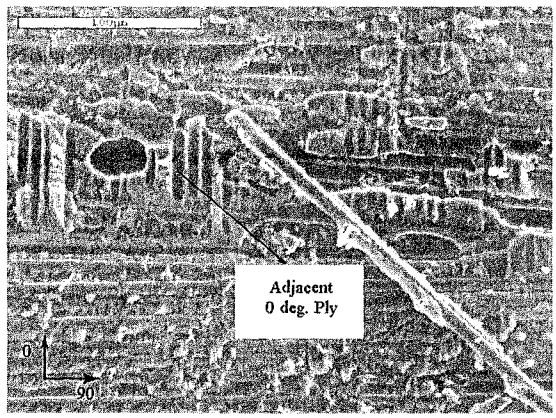

Fig. 8 SEM image showing 90D90 specimen crack surface

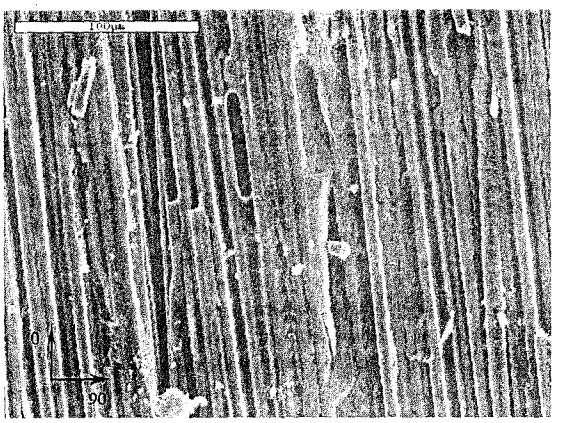

Fig. 9 SEM image showing 9% nanotreated specimen crack surface

the topographical difference between the two surfaces.

0D0_N_20 and 0D0 specimens show similar fracture toughness at room temperature, but at cryogenic temperature 0D0_N_20 specimen shows a slight improvement in G_{Ic} over 0D0 specimen indicating that nano treatment improves the fracture property of the composite. Also, comparison of 0D0_N_9 and 0D0_N_20 specimens fracture properties show that the amount of nanoparticles used is critical.

Fracture Toughness of Textile Composites. The textile composite specimens showed higher fracture toughness (422 N/m) compared to both the unidirectional (0D0 and 90D90) specimens. At cryogenic conditions the fracture toughness of the textile composite (TEX) specimens increased by nearly 96% compared to the room temperature specimen. Figure 6 shows the comparison of G_{Ic} of the unidirectional laminates and textile laminates.

Figure 10 shows the SEM photograph of the textile specimen crack surface. We can clearly see that there are numerous broken fibers on the surface of the crack. As mentioned earlier the increase in fracture toughness might be due to the fact that more energy is required to break the fibers. In the case of the cryogenic specimens it was observed that the crack growth was more translaminar than interlaminar, i.e., the crack growth was not planar and propagated through the adjacent plies. The increase in fracture toughness at cryogenic temperature might be due to this deviation in the crack path.

Conclusions

Double cantilever beam tests were performed at room and cryogenic temperatures on composite laminates to investigate the effect of cryogenic temperature on the fracture toughness. Different types of DCB composite specimens with the precrack between, two 0 deg plies, two 90 deg plies, 0 deg and 90 deg plies, and two textile plies were tested at room and cryogenic temperatures. Some of the specimens were treated with nanoparticles (38 nmAl_2O_3) at the ply interface, to determine its effect on the fracture toughness. The critical energy release rate G_{Ic} was calculated for each specimen using the area method.

Comparing the G_{Ic} values of the unidirectional specimens, we find that the 90D90 specimens exhibited higher fracture toughness compared to the 0D0 specimens. Also, both the specimens showed deterioration in fracture toughness at cryogenic temperature. The fracture toughness was least for the 90D0 specimens.

The results from nanoparticle treated composite specimens showed an improvement in fracture toughness at both room temperature and cryogenic temperature. Hence, the use of nanoparticles to improve fracture toughness should be considered in future applications. The amount of nanoparticles is critical as evidenced by the difference in fracture toughness between the 9% (0D0_N_9) and 20% (0D0_N_20) nanotreated specimens. More research needs to be done in the future to optimize the quantity of the nanoparticles that should be used and techniques to impregnate them into the composite.

Textile composites specimens exhibited good resistance to delamination at room temperature compared to the unidirectional specimens. The fracture toughness of the textile specimens almost doubled at cryogenic temperature. The results from this study points to the potential advantages of using textile composites for structures at cryogenic temperatures.

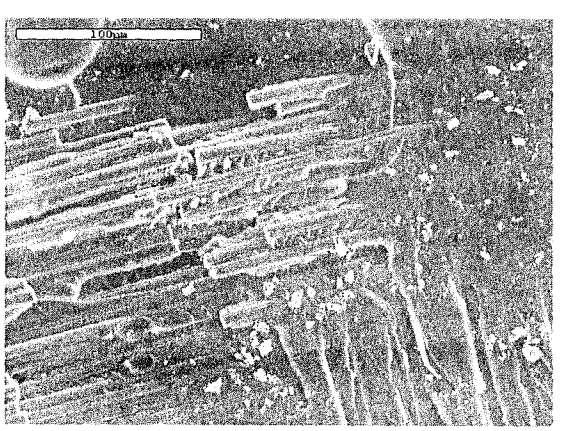

Fig. 10 SEM image showing TEX specimen crack surface

Acknowledgment

The authors gratefully acknowledge the technical and financial support of NASA Glenn Research Center (NAG3-2750) and NAG3-2750 NASA Kennedy Space Center under the Hydrogen Research and Education Program.

References

[1] Final Report of the X-33 Liquid Hydrogen Tank Test Investigation Team, 2000, Marshall Space Flight Center, Huntsville, AL, May.
[2] Grimsley, B. W., Cano, R. J., Johnston, N. J., Loos, A. C., and McMahon, W. M., 2001, "Hybrid Composites for LH2 Fuel Tank Structures," *Presented at 33rd International SAMPE Technical Conference*, November 4–8, Seattle, Washington, SAMPE, Covina, CA.
[3] Anderson, T. L., 1995, *Fracture Mechanics*, 2nd ed., CRC Press LLC, Boca Raton, FL.
[4] Sankar, B. V., and Sonik, V., 1995, "Point Wise Energy Release Rate in Delaminated Plates," AIAA J., **33**(7), pp. 1312–1318.
[5] Sun, C. T., and Zheng, S., 1996, "Delamination Characteristics of Double Cantilever Beam and End-Notched Flexure Composite Specimens," Compos. Sci. Technol., **56**, pp. 451–459.
[6] Davidson, B. D., Kruger, R., and Konig, M., 1996, "Effect of Stacking Sequence on Energy Release Rate Distributions in Multidirectional DCB and ENF Specimens," Eng. Fract. Mech., **55**(4), pp. 557–569.
[7] de Morais, A. B., de Moura, M. F., Marques, A. T., and de Castro, P. T., 2002, "Mode I Interlaminar Fracture of Carbon/Epoxy Cross-Ply Composites," Compos. Sci. Technol., **62**, pp. 679–686.
[8] de Morais, A. B., 2003, "Double Cantilever Beam Testing of Multidirectional Laminates" Composites, Part A, **34**(12), pp. 1135–1142.
[9] Ashcroft, I. A., Hughes, D. J., and Shaw, S. J., 2001, "Mode I Fracture of Epoxy Bonded Composite Joints: 1. Quasi-Static Loading," Int. J. Adhes. Adhes., **21**, pp. 87–99.
[10] Shindo, Y., Horiguchi, K., Wang, R., and Kudo, H., 2001, "Double Cantilever Beam Measurement and Finite Element Analysis of Cryogenic Mode I Interlaminar Fracture Toughness of Glass-Cloth/Epoxy Laminates," ASME J. Eng. Mater. Technol., **123**, pp. 191–197.
[11] Sharma, S. K., and Sankar, B. V., 1995 "Effects of Through-the-Thickness Stitching on Impact and Interlaminar Fracture Properties of Textile Graphite/Epoxy Laminates," NASA Contractor Report 195042.
[12] Wallace, B. T., Sankar, B. V., and Ifju, P. G., 2001, "Pin Reinforcement of Delaminated Sandwich Beams Under Axial Compression," J. Sandwich Struct.

Mater., **3**(2), pp. 117–129.
[13] Rys, T. P., Chen, L., and Sankar, B. V., 2004, "Mixed Mode Fracture Toughness of Laminated Stitched Composites," SEM X Paper 293, *Proceedings of the 2004 SEM X International Congress and Exposition on Experimental and Applied Mechanics*, Costa Mesa, CA.
[14] Wu, S. H., Wang, F. Y., Ma, C. C. M., Chang, W. C., Kuo, C. T., Kuan, H. C., and Chen, W. J., 2001, "Mechanical, Thermal and Morphological Properties of Glass Fiber and Carbon Fiber Reinforced Ployamide-6 and Polyamide-6/ clay Nanocomposites," Mater. Lett., **49**, pp. 327–333.
[15] Becker, O., Varley, R. J., and Simon, G. P., 2003, "Use of Layered Silicates to Supplementarily Toughen High Performance Epoxy-Carbon Fiber Composites," J. Mater. Sci. Lett., **22**, pp. 1411–1414.
[16] Timmerman, J. F., Hayes, B. S., and Seferis, J. S., 2002, "Nanoclay Reinforcement Effects on the Cryogenic Microcracking of Carbon Fiber/Epoxy Composites," Compos. Sci. Technol., **62**, pp. 1249–1258.
[17] ASTM D 5528-94a, 1996, "Standard Test Method for Mode I Interlaminar Fracture Toughness of Unidirectional Fiber-Reinforced Polymer Material Composites" Annual Book of ASTM Standards, 15.03, pp. 280–289.
[18] Kalarikkal, S. G., 2004, "Fracture Toughness of Graphite/Epoxy Laminates at Cryogenic Conditions," M.S. thesis, University of Florida, Gainesville, FL.